Investigation of recombination parameters in silicon structures by infrared and microwave transient absorption techniques

E Gaubas, A Kaniava and J Vaitkus

Institute of Material Science and Applied Research, Vilnius University,
Sauletekio 10, 2054 Vilnius, Lithuania

Abstract. Contactless techniques of infrared and microwave absorption by free carriers for the monitoring of silicon structures are described. Theoretical principles of photoconductivity decay analysis and methodology for the determination of recombination parameters are given for both homogeneous and non-homogeneous excess carrier generation. Different approximations (the methods of decay amplitude–asymptotic lifetime analysis, the simulation of the whole decay curve, the variation of effective lifetime with wafer thickness and the asymptotic lifetime measurement for stepwise varying parameters in layered structure) corresponding to real experimental conditions for various structures and treatments of materials, which are important for microelectronics, are discussed.

The determined recombination parameters in the range of bulk lifetime 0.0006–230 μs, velocity of surface recombination 600–5 $\times$ 10^4 cm s^{-1} and diffusion coefficient 0.015–18 cm^2 s^{-1} are illustrated for Si wafers obtained by various doping and preparation processes. The necessity to consider carrier trapping effects and nonlinear recombination processes is demonstrated by the analysis of experimental results obtained at different excitation levels for carrier concentrations in the range 10^{13}–10^{18} cm^{-3}. The possibility of extracting the parameters of the traps (with activation energy values 0.16 $\pm$ 0.02 eV, 0.20 $\pm$ 0.02 eV and 0.28 $\pm$ 0.04 eV) from the temperature-dependent asymptotic carrier lifetime measurements is illustrated for neutron transmutation doped wafers.

1. Introduction

Carrier lifetime is a basic electrophysical parameter of semiconductor material, which affects device characteristics and is most sensitive to structural perfection. The control of crystal growth and defects induced by device structure fabrication by contactless lifetime monitoring may be useful to govern the performance of semiconductor devices.

The effective recombination time (τ_{eff}) in the asymptotic part of carrier decay averaged over the thickness of the sample is conventionally measured [1–8]. This parameter is suitable when carrier lifetime is independent of the excess carrier concentration, defects are homogeneously distributed at low concentration within the depth of the wafer and the surfaces of the wafer are well passivated. Even in well fabricated and carefully processed material these requirements are only satisfied in the limited range of intensities of optical excitation. When these conditions are not fulfilled, interpretation of the effective lifetime becomes more complicated due to uncertainty

of a set of recombination parameters. Light-induced carrier concentration decay is defined by recombination on the surface and within the bulk. It also depends on the redistribution of carriers due to diffusion. Thus, simultaneous determination of diffusion constant (D), surface recombination velocity (s) and bulk lifetime (τ_b) is required. Additional problems arise when trapping effects at low injection level and Auger-type processes at high excitation are significant. For these nonlinear situations, as well as for the control of recombination parameters in layered silicon structures, combined experimental measurements and computer simulation are desirable.

There are some well known methods for determining carrier bulk lifetime and surface recombination rate [1–4]. Light-induced infared (IR) and/or microwave (MW) transient absorption are widely used methods for decay measurement. The recombination parameters are extracted from the excess carrier concentration (IR) or conductivity (MW) decay. Conventional methods for the separation of bulk lifetime and surface recombination velocity are

usually based on the dependence of the effective lifetime on the thickness of wafer [1]. For the direct evaluation of long bulk lifetimes ($\tau_b > 100\ \mu$s) it is necessary to additionally passivate both surfaces of the wafer to suppress surface recombination [5–7]. In many cases, however, one is also interested in knowing the surface recombination lifetime. Computer simulation of the carrier concentration amplitude–time characteristics [9–11] is a powerful technique for the extraction of both recombination parameters which requires extensive calculations.

In this paper some experimental situations and photoconductivity decay modelling problems are discussed on the basis of investigations performed on various batches of Si wafers. The asymptotic and/or instantaneous decay time is considered as the experimental parameter for the first order of approximation of different types of recombination nonlinearities. The algorithms for the extraction of recombination parameters, which extend the consideration of this type of problem [9, 10], are presented. The methodologies of the express contactless monitoring of material by infrared as well as microwave transient absorption are analysed.

2. Theoretical principles

2.1. Extraction of the parameters of linear recombination

Excess carrier concentration averaged over the thickness of wafer is determined by the analytical solution of the unified (for both types of carriers) linear continuity equation:

$$\partial n/\partial t = D\,\partial^2 n/\partial^2 x - n/\tau_b \quad (1)$$

$$D\,\partial n/\partial x|_{x=0,d} = \pm s_{1,2}n|_{x=0,d} \quad (1a)$$

$$n|_{t=0} = n_0 \exp(-\alpha d). \quad (1b)$$

The solution is expressed as a series of space frequency ν_m constituents:

$$\langle \Delta n\rangle_d = \Delta n_0 \sum_{m=1}^{\infty} A_m^* \exp[-(\nu_m^2 D + \tau_b^{-1})t] \quad (2)$$

and the space frequency ν_m is determined by the solution of the transcendental characteristic equation:

$$\cot \nu d = \frac{D\nu}{s_1 + s_2} - \frac{s_1 s_2}{(s_1 + s_2)D\nu}. \quad (3)$$

The amplitude coefficients in the solution (equation (2)) are expressed as follows:

$$A_m^* = \{8\,e^{-\alpha d/2} \sin^2(\nu_m d/2)[\alpha\sinh(\alpha d/2)\cos(\nu_m d/2)$$
$$+\nu_m \cosh(\alpha d/2)\sin(\nu_m d/2)]\}$$
$$\times\{d(\alpha^2 + \nu_m^2)(\nu_m d + \sin \nu_m d)\}^{-1}. \quad (4)$$

Here s_1, s_2 are the velocities of the surface recombination on the front and rear side of wafer respectively. The transitional part of the decay kinetic, described by the sum of ν_m constituents, is non-exponential due to the different influence of the higher space frequencies on various stages of the relaxation process. The expression for the amplitude

coefficients A_m^* coincide with that obtained in [1], but these values are not experimentally measured.

The excess carrier concentration $n(t)$, averaged over the thickness d of wafer and normalized to that of the initial carrier concentration $n(0)$ (i.e. $\langle n(t)\rangle_d/\langle n(0)\rangle_d$) is expressed by modified amplitude coefficients

$$A_m = \frac{2\alpha d\,\sin(\nu_m d)[\alpha d + \nu_m d\tan(\nu_m d/2)\coth(\alpha d/2)]}{[(\alpha d)^2 + (\nu_m d)^2][\nu_m d + \sin(\nu_m d)]}. \quad (5)$$

The amplitudes A_m are normalized to unity at $t = 0$ by $\sum_{m=1}^{\infty} A_m = 1$. The normalized amplitude of the main decay mode A_1 can be experimentally determined by extrapolation of the asymptotic decay part to the initial moment. It may serve as a quick method for the separation of the parameters of bulk and surface recombination [12]. A similar method is proposed in [9], although it requires a more complicated simulation.

The simple nomographic method [12] briefly presented here enables one to address the spatial variations of carrier concentration through $\nu_m d$ and the surface recombination by measuring the absolute value of the decrease of he amplitude A_1. The principle is based on the experimental determination of normalized carrier concentration $\sum_{m=1}^{\infty} A_m \exp[-t_M(\tau_b^{-1} + \tau_{sm}^{-1})]$ which cannot decrease below $A_1\exp(-t_M/\tau_{eff})$ at the moment of observation t_m. Here $\tau_{sm} = 1/\nu_m^2 D$ are decay constituents of the surface recombination and $\tau_{eff}^{-1} = \tau_b^{-1} + \tau_{sl}^{-1}$. This allows A_1 to be determined experimentally and, consequently, $\nu_1 d$ to be obtained from (5). The A_1 dependences on $\nu_1 d$ for different excitation decrements αd are presented in figure 1. These dependences may serve as a nomographic method for the determination of $\nu_1 d$ from the experimentally measured values of A_1. The amplitudes are thus determined by αd and $\nu_m d$. Therefore the amplitudes A_m depend on both boundary and initial conditions. The impact of absorption inhomogeneity is most significant for the lower modes. In this case values of $\nu_m d$ for low modes may be significantly smaller than αd in (5), i.e. A_1 is relatively lowered with increasing αd, while A_m for the highest modes is increased with αd or is nearly independent of αd (for $\alpha d/\nu_m d \to 1$).

On the other hand, the duration of the non-exponential transitional part of the carrier concentration decay (τ_{tr}) can be evaluated taking into account the experimental error ε. The higher modes can be neglected when these constituents $A_m \exp(-t_M/\tau_{sm})$ are smaller than the fluctuations of the main mode $\varepsilon A_1 \exp(-t_M/\tau_{sl})$ caused by experimental error. Thus, the asymptotic decay part is achieved at

$$\varepsilon A_1 \exp(-\tau_{tr}/\tau_{sl}) = \sum_{m=2}^{\infty} A_m \exp(-\tau_{tr}/\tau_{sm}) \quad (6)$$

which for $\varepsilon \approx A_2$ and for $\varepsilon A_1\exp(-\tau_{tr}/\tau_{sl}) \approx A_2\exp(-\tau_{tr}/\tau_{s2})$ reduces to

$$\tau_{tr} \approx \frac{\tau_{sl}|\ln A_1|}{\tau_{sl}/\tau_{s2} - 1}. \quad (7)$$

The decay times τ_{sm} hinge only on the boundary conditions (as $\tau_{sm} \propto \nu_m^{-2}$) and are not influenced by the excitation conditions (because are only determined by (3)).
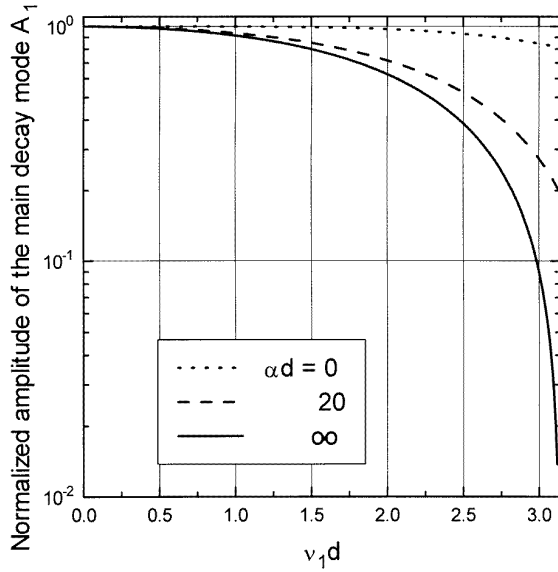
Figure 1. The thickness averaged and normalized carrier concentration as the amplitude of the main mode versus modulation depth $v_1 d$ for homogeneous ($\alpha d = 0$), inhomogeneous ($\alpha d = 20$) and surface ($\alpha d = \infty$) excitation.

The approximations of the solution of the characteristic transcendental equation (3) are useful for express data processing in more general situations when higher decay modes should be taken into consideration. In the case of negligible surface recombination on one side of wafer (e.g. $s_2 = 0$) only the first constituent of equation (3) (right part) remains and equation (3) transforms to

$$\cot v d = Dv/s. \qquad (8)$$

The solution of the reduced equation is governed either by the surface recombination, when $D/s > d$, or by the diffusion, when $d < D/s$. The unidirectional diffusion to the face surface (s_1) appears when $s_2 = 0$. For the widely used approximation of equal surface recombination rates $s_1 = s_2 = s$, the transcendental equation (3) is also transformed to the reduced one (8) when the wafer thickness d is formally changed to $d/2$: i.e. the bidirectional diffusion, due to its symmetry, is replaced by the consideration of unidirectional diffusion. The solution $v_m d$ of the reduced equation (which depends on the ratio $L = D/sd$) can be approximated by functions $F(Y = L)$:

$$F_1(Y) = \left[\!\!\left[\tfrac{15}{2}(3Y + 1)\{[1 + \tfrac{4}{5}(3Y + 1)]^{1/2} - 1\}\right]\!\!\right]^{1/2}$$
$$\text{for } m = 1$$

$$F_m(Y) = \pi \frac{3Y}{3Y + 1}\left[\left(1 + \frac{4}{3Y^2(m-1)^2\pi^2}\right)^{1/2} - 1\right]$$
$$\text{for } m \geq 2. \qquad (9)$$

The solution $v_1 d$ in fact represents the cut-off angle of the carrier concentration $n_s \propto n_0 \cos v_1 d$ on the wafer surface or at the virtual boundary where the opposite flows of carrier diffusion are compensated for

$v_m d$ within distances $v_m^{-1} = \sqrt{Dt}$, and is expressed as follows:

$$v_1 d = F_1(L)$$
$$\text{when } L > 0.04 \text{ and } F_1 \approx L^{-1/2} \text{ for } L \to \infty, s \to 0$$

$$v_1 d = (\pi - F_1(L^{-1})/2)/2$$
$$\text{when } L \leq 0.04 \text{ and } F_1(L^{-1}) \approx L^{1/2} \text{ for } L \to 0$$

$$v_m d = (m - 1)\pi + F_m(L)$$
$$\text{when } L > 0.1 \text{ and } F_m(L) \to 0 \text{ for } L, m \to \infty$$

$$v_m d = (m - 0.5)\pi - F_m(L^{-1})$$
$$\text{when } L < 0.1 \text{ and } F_m(L^{-1}) \to 0 \text{ for } m \to \infty. \qquad (10)$$

It can be noticed that $v_1 d$ decreases to zero when the ratio L infinitely increases due to $s \to 0$, and it increases to $\pi/2$ when $L \to 0$ due to $s \to \infty$. The $v_1 d = \pi/2$ is the upper limit value for unidirectional diffusion to the surface. The faster approach of $v_m d$ to its limit value of $m\pi$ is achieved for the higher mode numbers m. The latter value is inherent to the exact solution of the continuity equation with the boundary conditions $s_1 = s_2 = \infty$.

The quantity $v_1 d$ as a function of the generalized parameter $L_{d/2} = 2D/sd$ for the main decay mode can be approximately expressed for symmetric surface recombination as follows:

$$v_1 d = 2/\{L_{d/2} + [\pi/2 + (1/9)L_{d/2}^{1/2}]^{-2}\}^{1/2}. \qquad (11)$$

Here the weight coefficient $\propto \pi^{-2}$ is replaced by $1/9$ due to neglected higher modes. This solution is compared with the direct solution of the transcendental equation (8) in figure 2. The heuristic evaluation of the first root of the transcendental equation (8) by the widely used [14] approximation $\tau_{sl} = \tau_{s\to0} + \tau_D$ (where $\tau_{s\to0} = d/2s$ and $\tau_D = d^2/\pi^2 D$) is presented in figure 2 also. The discrepancies between the exact solution and the latter approximation give rise to errors of more than 2% in $v_1 d$ and more than 4% in τ_{sl} for $L_{d/2} > 1$. Approximation (11) is enough to get an estimation of $v_1 d$ with errors less than 1% in the whole range of $L_{d/2}$.

For asymmetry of surface recombination rates, for example $s_1 > s_2$, equation (3) can be approximated by a reduced one in which s is replaced by the sum $s_1 + s_2$ for $L > 1$. The maximum of the stabilized excess carrier concentration in the asymmetric case is shifted towards the slower surface recombination side when $d\sqrt{s_1 s_2}/D \leq \pi/2$. The position of this maximum from the surfaces of the wafer is defined by the distances d_1 and d_2 when it is postulated that $d_1/d_2 = s_1/s_2$ and $d_1 + d_2 = d$. Thus, $d_1 = d/(1 + s_2/s_1)$. Then equation (3) transforms as follows:

$$\cot v d = (Dvd/s_1 d_1)(d_1/d_2)^2 - s_1(d - d_1)/Dvd. \qquad (12)$$

The solution of (12) can be expressed by the function $F_{12}(L_1, L_2)$:

$$F_{12}(Y_1, Y_2) = \{\tfrac{15}{2}(3Y_1 + 1)$$
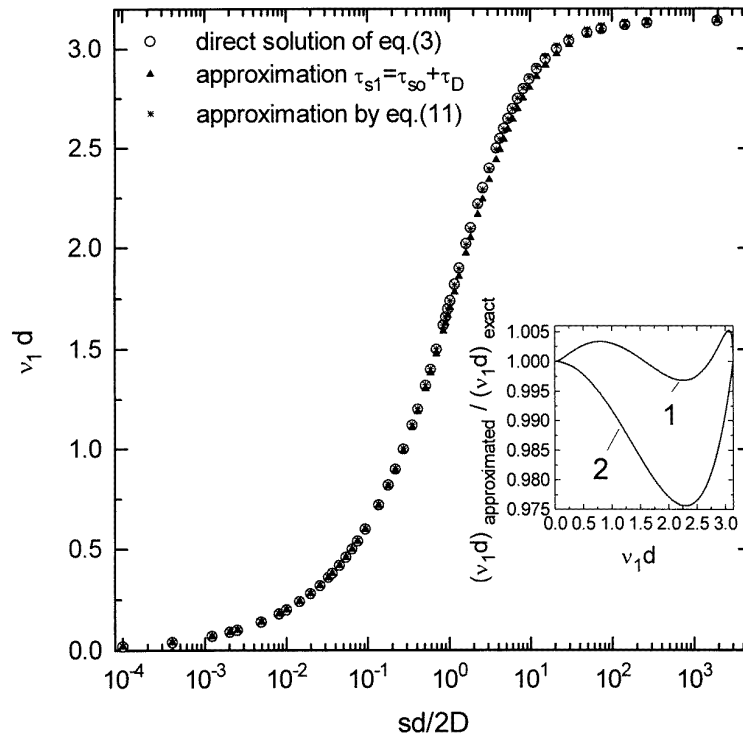$$\times [\langle 1 + 4(Y_2 + 1)/5(3Y_1 + 1)^2\rangle^{1/2} - 1]\}^{1/2} \qquad (13)$$

Figure 2. Modulation depth v_1d for the main decay mode versus generalized parameter $sd/2D$ obtained by direct solution of the transcendental equations (3), (8), approximated by equation (11)—curve 1 in the insert—and by sum of limiting surface recombination times—curve 2 in the insert.

and the reduced ratios $L_1 = (D/s_1d_1)(d_1/d)^2$, $L_2^{-1} = D/s_1(d - d_1)$. The cut-off angle v_1d of the carrier distribution profile can be expressed by the function F_{12} with different arguments:

$$v_1d = F_{12}(L_1, L_2) \text{ when } Q = d\sqrt{s_1s_2}/D < 1$$

$$v_1d = \pi/2 - F_{12}(L_1^{-1}, L_2^{-1}) \text{ for } 1 < Q \le \pi/2. \quad (14)$$

Thus, the space frequency for the stabilized carrier distribution and for $Q < 1$ can be expressed as $v_1 = (s_1/d_1D)^{1/2}$. The effective distance d_1 can be determined either by measuring the probing depth in the reflection mode for which the saturation of the averaged concentration is achieved or by perpendicular scanning of the concentration profile by the method proposed in [2]. Measuring d_1 and obtaining the value of v_1 from A_1 and τ_{eff}, the velocity of surface recombination s_1 can be calculated. Afterwards s_2 is determined through s_1, d_1.

Either the surface recombination rate or the diffusion coefficient can be extracted from the τ_{eff}^{-1} dependence on the wafer thickness d for limiting conditions of $s \to 0$ or of $s \to \infty$. In the intermediate cases the exponent index χ of the characteristic $\tau_{\text{eff}}^{-1}(d^{-\chi}) = \tau_b^{-1} + F^2(D, s, d)D/d^2$ is in the range of $1 < \chi < 2$. The extrapolation of this function to $d = \infty$ allows us to evaluate τ_b, and then either D or s can be estimated from the slope of the characteristic $\tau_{\text{eff}}^{-1}(d^{-\chi})$ depending on which process is dominant.

The asymptotic decay time τ_{eff} can be considered as a sufficient approximation of inhomogeneous structure. In this case, the effective lifetime τ_{eff} is measured as an

instantaneous recombination time τ_M for the slowest part of decay, and it may be described by approximation of the effective thickness [13]. The impact of excitation depth on the instanteous lifetime is approximately expressed by the relation $\tau_M \propto \alpha^{-2}$. In the case of a layered structure the effective lifetime can be considered through assumed stepwise varied recombination parameters [11, 13]. This approximation also assumes that the initial carrier concentration is generated only in the range of light penetration depth. For analysis of the two-layer structure, consisting of the implanted layer and substrate, the continuity equation is considered with stepwise changing coefficients: d_1, τ_1, s_1, D_1 and d_2, τ_2, s_2, D_2 for the implanted layer and substrate respectively. This task is solved with typical boundary conditions accounting the surface recombination as well as conjugation conditions at the structure interface, i.e. assuming equality of the diffusion flows and excess carrier concentrations on it. The differential equation may be solved by the method of the separation of variables, and the concentration averaged over the effective thickness is presented by the expression

$$\langle \Delta n \rangle_d = \Delta n_0^* \sum_{j=1}^{2} \sum_{m=1}^{\infty} \exp(-\eta_m t)$$

$$\times (8L_{jm} \sin^2 y_{jm}/2d_{\text{eff}})/(y_{jm} + \sin y_{jm}) \quad (15)$$

where Δn_0^* is the initial excess carrier concentration, $L_{jm} = [D_j/(\eta_m - \tau_j^{-1})]^{1/2}$, $y_{jm} = d_j/L_{jm}$ are characteristic and normalized depths for each layer j and mode m. The effective lifetime is determined by $\tau_{\text{eff}} = \eta_1^{-1}$, and η_m is

the root of the transcendental equation. In the case of long bulk lifetimes it is expressed as follows:

$$\frac{p_1(q_1 + \tan y_1)}{1 - q \tan y_1} = p_2 \cot\left(\frac{d_{\text{eff}} - d_1}{L_2}\right). \qquad (16)$$

Here $p_j = L_j/D_j$, $q_j = D_j/L_j s_j$. This solution formally correlates with the solution for a homogeneous sample with $d_1 = 0$ and $d_{\text{eff}} = d$ as well as with the solution for the homogeneous excitation of the two-layer structure when the real carrier distribution profile is approximated by a rectangular one with the average concentration Δn_0^*. The solution (16) presented above is valid when the difference between the bulk lifetimes τ_j in the implanted layer ($j = 1$) and substrate ($j = 2$) is small and the surface recombination prevails. If the bulk lifetimes in the implanted layer is the smallest among the other recombination times the transcendental equation acquires the form

$$\frac{p_1^*(1 + r_1)}{1 - r_1} = p_2 \cot\left(\frac{d_{\text{eff}} - d_1}{L_2}\right) \qquad (17)$$

where $L_{1m}^* = [D_1/(\tau_1^{-1} - \eta_m^*)]^{1/2}$, $p_1^* = L_{1m}^*/D_1$, $r_1 = \exp(-2y_1^*)(D_1 - s_2 L_1^*)/(D_1 + s_1 L_1^*)$. Although the expression for the averaged concentration (equation (15)) acquires a slightly different form (sin $\to$ sinh), the time evolution of carrier concentration is characterized by η_m^* and remains the same. In order to be able to extract the recombination parameters both in the implanted layer and in the substrate by measurement of the asymptotic relaxation times at different excitation depths the main task is to solve transcendental equations (16) and (17). A computer simulation procedure to achieve the best fit of measured and calculated asymptotic lifetimes at different excitation depths for the same sample includes consideration of transcendental equations (16) and (17). The fitting procedure for such a structure of the implanted layer-substrate is illustrated in figure 3.

2.2. Nonlinear recombination

A more general model for determination of the recombination parameters including the nonlinear recombination due to carrier trapping and Auger-type process is based on the solution of the system of one-dimensional continuity equations (separate for electrons n and holes p):

$$\partial n/\partial t = D_n \partial^2 n/\partial x^2 - n/\tau_n - n/\tau_q + q/\tau_g - \gamma_j n^j \quad (18a)$$

$$\partial q/\partial t = n/\tau_q - q/\tau_g \qquad (18b)$$

$$\partial n/\partial x|_{x=0,d} = \pm s_{0,d} n/D_n \qquad (18c)$$

$$n|_{t=0} = n_0 f(x), \; q|_{t=0} = q_0 \qquad (18d)$$

$$q + n = r + p \qquad (18e)$$

with boundary (18c) and initial (18d) conditions. Here the equations for excess electrons are presented, and the same equations must be added for holes by replacing $p \to n$, $r \to q$, where q is the concentration of trapped carriers. These equations are conjugated by a neutrality equation (18e). The notation is standard: τ_n, τ_q, τ_g are carrier lifetimes relating to recombination, trapping and
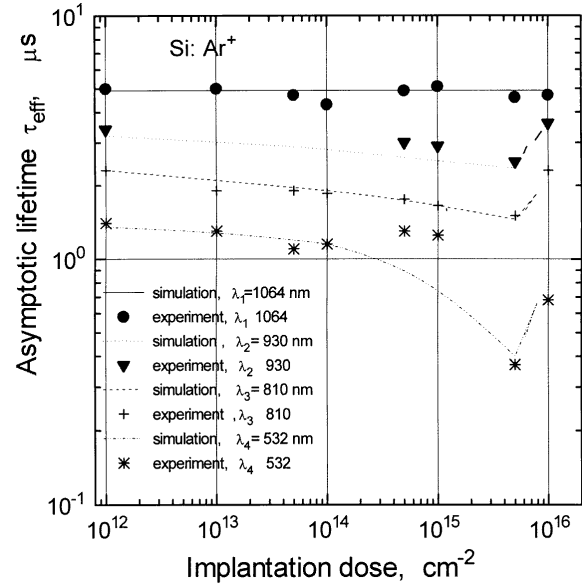

Figure 3. Simulated and experimental asymptotic lifetime dependence on the dose of implanted ions for the structure of implanted layer–substrate.

thermal generation respectively, γ_j are the coefficients of nonlinear Auger-type recombination ($j = 2, 3, \ldots$). This system must be solved numerically, when the trapping effects are significant. Experimental selection of the dominant processes as well as their parameters at fixed range of injection levels $\beta = (\Delta n + \Delta p)/(n_0 + p_0)$ is necessary. The recombination process is described by the unified ($n = p$) equation (18a) and unified instantaneous time τ_M if trapping can be neglected. The experimental decay data are compared with numerically simulated curves for such a situation of simultaneous action of the SRH and Auger processes of nonlinear recombination in figure 4.

The instantaneous relaxation time τ_M at the moderate injection level $\beta \geq 1$ even in the case of recombination via a single level (with small concentration of centres) depends on the excess carrier concentration [15, 16]:

$$\tau_{M\,SRH} = \frac{\tau_0 + \beta \tau_\infty}{1 + \beta}. \qquad (19)$$

Consequently, the decay process is non-exponential due to $\beta(\Delta n(t))$. Here τ_0 is the recombination time at a low injection level, which contains a dependence on the temperature as well as on the activation energy of the centre. The time τ_∞ of the high injection level is only dependent on the temperature via a temperature-dependent carrier capture cross section. The validity of the well known SRH model can be estimated by the linearity of the dependence of $\tau_{M\,SRH}(1 + \beta) = f(\beta)$. τ_0 and τ_∞ can be obtained from this linear dependence, and the SRH model (for a single-type centre) cannot be applied, when this characteristic is nonlinear. The experimentally measured asymptotic time τ_{eff} represents the parameter τ_M, which changes with β in the range between τ_0 and τ_∞. The activation energy of the recombination of defects can be found by measurements of the dependence of $\tau_{M\,SRH}$ on
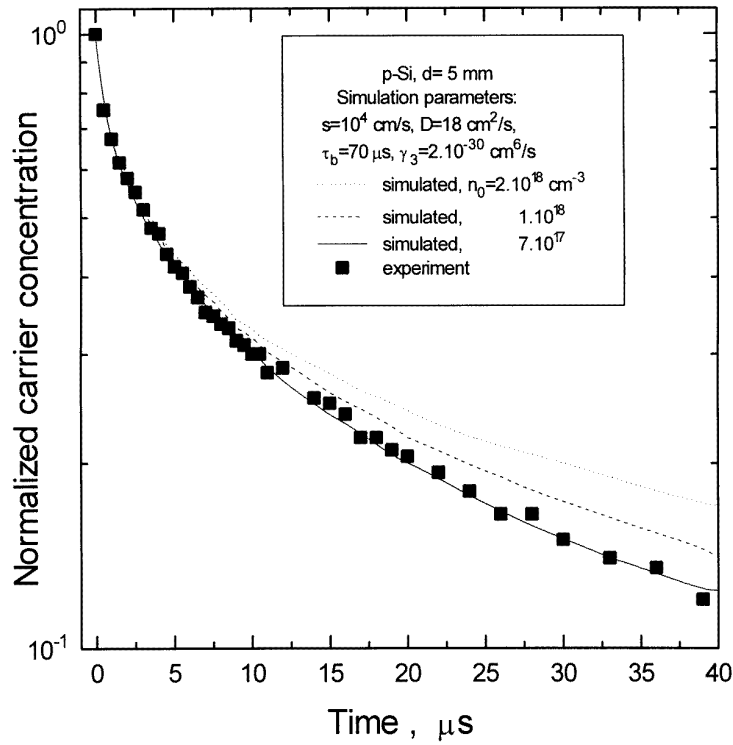
5

Figure 4. Simulated and experimental decay kinetics in the presence of nonlinear recombination.

temperature, when $\tau_0 \geq \beta\tau_\infty$ and carrier generation from impurities is saturated. $\tau_{\text{eff}}(T)$ will be distorted by changes in $\beta(T)$ in other cases.

The reason for discrepancy from the linear dependence (equation (19)) of $\tau_{\text{M SRH}} = f(\beta)$ could be the carrier trapping effect caused by the large concentration of defects (M). The main feature of this process is inequality of the concentration of excess electrons and of holes ($\Delta n \neq \Delta p$) [15, 16]. The asymptotic time will be determined by the longest of the partial times (τ_n, τ_p). As a rule carriers of one type are trapped, and their lifetime is the shortest. Inequality of the lifetimes and concentration of excess carriers leads to the concentration-dependent diffusion coefficient [15]: $D = (n + p)/(n/D_p + p/D_n)$.

Carriers trapping gives complementary information about the defects in material. The trapping disappears in the case of the stationary excitation due to compensation of the flows of carrier capture/re-emission. Consequently, additional stationary illumination (AI) can efficiently compensate these flows and considerably change the decay characteristics. A large variety of trapping centres (slow as well as fast) is known [15, 17]. The instantaneous recombination time for the multitrapping centres can be expressed as follows:

$$\tau_{\text{Mtr}} = \tau_n[1 + MN_{\text{CM}}/(\Delta n + n_0 + N_{\text{CM}})^2]. \qquad (20)$$

Here τ_n is the recombination lifetime of the trapped carriers, M is the concentration of traps, N_{CM} is the effective density of states. The instantaneous time saturates when $\Delta n \to 0$, and the trapping effect vanishes when Δn is large. Thus, the trapping coefficient $K = M/N_{\text{CM}}$ can be found from

changes in τ_{eff} versus excitation (or calibration of AI) at $\Delta n \to 0$, and τ_{eff}/τ_n dependence on the temperature enables us to obtain the activation energy of traps E_M. The most important feature of the above analysed trapping is the decrease of τ_{Mtr} with increasing excess carrier concentration as well as with switching on the steady-state additional illumination.

The opposite type of trapping effect (i.e. increasing of τ_{eff} both with excitation intensity and AI) can also be found. This effect is attributed to the activity of the extended defects assuming that their cross section σ is dependent on the carrier concentration due to their charge state. The screening of charges on the defect is determined by carriers of the matrix material. The instantaneous lifetime for trapping at the spherical defects can be expressed as follows:

$$\tau_{\text{Mtr}} = \tau_n[1 + (\varepsilon\varepsilon_0 \, kT/\sigma_0 e^2 \Delta n)^{1/2}]^{-2} \qquad (21)$$

and $\tau_{\text{Mtr}} \propto \tau_n \Delta n/kT$, when $\sigma/\sigma_0 \gg 1$. Here e is an elementary charge and σ_0 is the intrinsic cross section. The increase of τ_{Mtr} with excitation and AI may be explained by a decrease of the screening radius at higher carrier concentrations. The decrease of τ_{Mtr} with Δn saturates when the recombination efficiency of other recombination centres starts to dominate the relaxation process, and it increases with Δn until the cross section decreases to the geometrical one of the extended defect. The geometrical cross section σ_0 can be evaluated by this model from $\tau_{\text{Mtr}}(\Delta n)$.

The simultaneous appearance of surface and bulk recombination including nonlinear recombination/trapping

processes requires the introduction of different instantaneous and asymptotic lifetimes from those presented by (19)–(21) as well as τ_n, τ_p, $\tau_A = 1/\gamma_3\Delta n^2$ and $\tau_{eff} = (\tau_b^{-1} + \tau_{sl}^{-1})^{-1}$ respectively. The instantaneous lifetime is traditionally [15, 16] defined as $\tau_M = -\Delta n/(\partial n/\partial t)$. It can characterize the rate of the recombination/decay process. The instantaneous lifetime τ_M defined in this way coincides with the bulk recombination lifetime τ_b, which is also characteristic of the material, if surface recombination and the above-mentioned nonlinearities of bulk recombination can be neglected. In the discussed cases of $\tau_{SRH}(\beta)$, of trapping effects and of nonlinear Auger recombination, the instantaneous lifetime enables one to compare the rate of recombination at different decay stages and, thus, to determine the dominant process. Although τ_M is not a material parameter in the latter situations, the instantaneous lifetime becomes constant in the asymptotic part of decay at the presence of surface recombination, when the sum in (2) vanishes, and separation of τ_{tr} and of τ_{eff} can be made through equations (6), (7) according to experimental error. Also, the changes of τ_M caused by nonlinear processes decrease in the asymptotic part of the decay. Thus, the asymptotic lifetime τ_{eff} defined as $\tau_{eff} = \tau_M|_{t\to\infty}$ is traditionally measured to characterize material through a quasilinear decay process. Therefore, the dependence of τ_M as well as τ_{eff} on the excitation level has to be investigated and used for the parameter extraction procedure by the presented techniques of amplitude–effective lifetime analysis, the $\tau_{eff}(d)$ dependencies or simulation of the whole decay curve.

Simultaneous determination of the set of recombination parameters is based on the adjustment of experimental and calculated characteristics by the least squares method. Analytical solutions of the bipolar continuity equation are used to determine the surface and bulk recombination parameters. To account for Auger-type recombination the excess carrier concentration decay is numerically simulated by the method of finite elements.

3. Experimental procedure

Measurement of the excess carrier decay characteristics is performed in the conventional pulse excitation/cw probe mode. Solid state and dye lasers as well as LED pulse radiation with discrete wavelengths λ in the range of 0.53–1.06 μm are used as the excitation light sources. The pulse duration is in the range of $\tau_L = 10$–100 ns to satisfy the approximation of a δ-pulse. The absolute values of excess carrier concentration are obtained by the calibrated measurements of the light energy density per pulse and used for the consideration of the nonlinear processes. However, the recombination parameters are necessary for more precise determination of light-induced carrier concentration (Δn). Thus, the absolute values of Δn are obtained by the iteration procedure.

Either the infrared (IR) radiation of a cw He–Ne ($\lambda = 1.15$ μm) laser or microwaves (MW) of 10 and 21 GHz are used to probe the excited area of the sample. The response

U of IR absorption by free carriers may be presented as follows:

$$U = k\{(1 - R)I_p \exp(-\sigma_\lambda n_0 d)[1 - \exp(-\sigma_\lambda \Delta n d)] - I_n\}. \tag{22}$$

Here I_p is the intensity of probe radiation, I_n is the noise intensity, d is wafer thickness, R is the reflection coefficient, n_0, p_0 are the concentrations of equilibrium electrons and holes and Δn, Δp of excess ones, and σ_λ is the effective cross section of absorption by free carriers at the probe wavelength λ. As the angle of incidence of the probe beam is the Brewster angle in our experiments, the impact of multiple reflections can be neglected. The coefficient k is the transfer function of the optical/electrical signal of detector.

To enhance the dynamic range of the instrument it is required that the intensity of the probe I_p be large, although the upper limit of I_p is restricted by the condition of the probe mode (i.e. $\Delta n_p/\Delta n_{ex} < 1$) and by the requirement to avoid heating of the material. Data preselection and statistical data processing are used to minimize the noises I_n. As σ_λ is the same for equilibrium and excess carriers, and wafer resistivity and thickness are fixed; the optimum of the response can be obtained at $\sigma_\lambda n_0 d = \ln(1 + \beta)/\beta$, and for $\sigma_\lambda n_0 d > 1$ the only compromise is to enlarge I_p. In other cases U decreases to kI_n. In our experiments the measurements are reliable for wafers with thickness $d \geq 50$ μm and resistivity of > 0.05 Ω cm for IR and > 2 Ω cm for MW probes respectively.

A relaxation curve usually consists of two main parts: the transitional (after short pulse excitation) nonexponential part and the quasi-exponential asymptotic one. The transitional part may be significantly modified by the presence of trapping effects. The asymptotic part (in our case measured at < 0.1 of the signal amplitude U_m), is approximated by the exponent. For reliable measurements of the asymptotic lifetime τ_{eff} was determined within a fixed range 0.1–0.02 of response amplitude U_m. Both the instantaneous times (for quasilinear approximation) and complete decay curve were recorded for further adjustment of calculated and experimental data. Variation of τ_{eff} within a linear increase of U_m is usually caused by the nonlinearity of recombination processes within the wafer. Linearity of the response amplitude can be found within 2.5 orders of $U_m(E_{ex})$ variation.

Most features of the experimental restictions for a MW probe are similar to those mentioned above for an IR probe. In this case the transient photoconductivity response may be expressed by the changes of quality factor (Q) of the MW waveguide/sample system, and Q is proportional to the resistivity of the sample.

4. Separation of bulk and surface recombination parameters

Figure 5 shows the τ_{eff} dependences on the excitation energy per pulse for double-side polished and etched p-Si 12 Ω cm wafers with different thicknesses in the range of 0.4–5 mm measured by the MW technique. Wafers were sliced from the same part of the ingot and
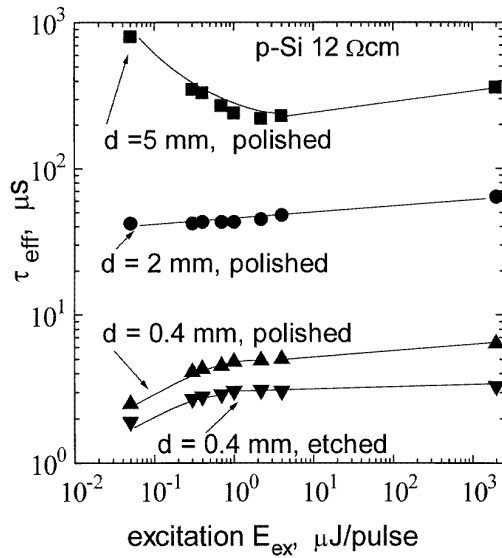
Figure 5. Dependence of asymptotic lifetime on excitation intensity and wafer thickness in p-Si 12 Ω cm.

Figure 6. Asymptoic lifetime versus wafer thickness measured at different excitation levels.

prepared by the identical procedure. Approximately the same recombination parameters s, τ_b are obtained from the analysis of A_1 and τ_{eff} as well as by fitting of the whole decay curve (figure 4) for the relatively thin wafers. As can be seen, the τ_{eff} dependence on the wafer thickness is different for low, moderate and high excitation levels. The recombination processes within the near-surface space charge region (SCR) are important for thin wafers, and τ_{eff} increases with E_{ex}. For thick wafers the trapping effect is significant, and τ_{eff} decreases versus E_{ex}. Thus, bulk lifetime can be directly measured in a thick wafer, $d \geq$ 5 mm, at the moderate excitation level ($E_{\text{ex}} \geq 10\ \mu$J/pulse). The dependence of τ_{eff} on E_{ex} of the etched wafer with rough surfaces illustrates inhomogeneity of bulk lifetime and the surface recombination for thin samples.

Figure 6 presents the characteristics $\tau_{\text{eff}}^{-1} = f[(\pi/d)^2]$ for different excitation energies to analyse the possibilities of parameter determination from the dependences of the effective lifetime on wafer thickness. The illustration of decay transient and asymptotic lifetime dependences on excitation level for this material are presented in figures 4 and 5. The argument of the function $\tau_{\text{eff}}^{-1} = f[(1/d)^\chi]$ as $(\pi/d)^2$ is chosen to determine the carrier diffusion coefficient. The linear dependences on a log/log scale are obtained for moderate excitation levels ($2 < E_{\text{ex}} <$ 200 μJ/pulse). The impact of the surface recombination on the integrated parameter τ_{eff} decreases with sample thickness. The lines are almost parallel for the thin wafers, but deviate from each other when the thickness exceeds 2 mm. The origin of the deviation is the injection-level-dependent bulk lifetime. At low excitation level τ_{eff}^{-1} decreases more quickly. It is determined by the competition between the surface recombination and carrier trapping: at high excitation level τ_{eff}^{-1} decreases more slowly and is mainly influenced by nonlinear recombination and the dependence of the diffusion coefficient on the carrier concentration. The slope in the linear part of the
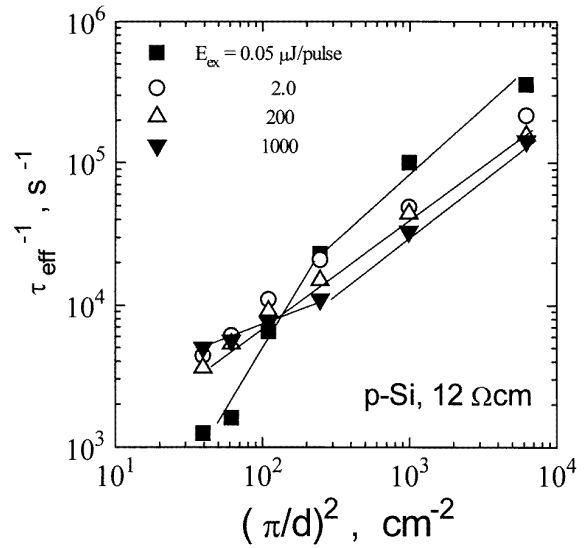
characteristics ($d < 2$ mm) for moderate and high excitation is nearly the same (in the range of intermediate values $\chi \approx 1$ and $\chi \leq 1.3$ respectively). The obtained χ values correlate with those predicted by the theoretical analysis. The constant slope (but different from the limited cases of $\chi - 1$ or 2) shows that diffusion–recombination processes are independent of the carrier concentration. On the other hand, the surface recombination velocity may be evaluated, if $\chi \approx 1$, and it is about $s \approx 4 \times 10^3$ cm s^{-1}. This value of s is in reasonable agreement (taking into account the excitation level) with that obtained from the fitting procedure of the decay curve (table 1).

At high excitation levels the Auger process is also efficient (figures 4 and 6), and band-to-band Auger recombination constant $\gamma_b = 2 \times 10^{-30}$ cm^6 s^{-1} was determined by decay curve analysis; it nearly coincides with that determined in [10, 18]. The thickness averaged bulk lifetime was found to be $\tau_b = 160\ \mu$s (at moderate excitation level) by extrapolation of the characteristic $\tau_{\text{eff}}^{-1} = f[(\pi/d)^2]$ to $d = \infty$.

The influence of the surface preparation and density of dislocations, intentionally introduced by the static deformations in the bulk of wafer, are also illustrated by τ_{eff} data in table 2. The asymptotic lifetime in an as-grown, freshly cut wafer was found to be 3.6 μs.
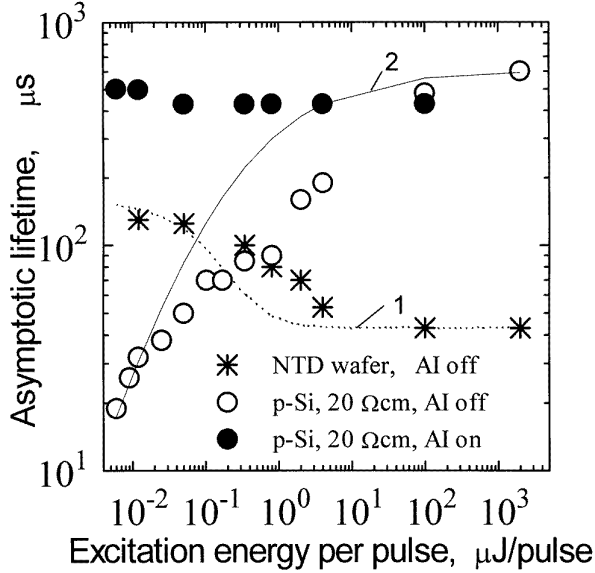
The set of recombination parameters at different excitation levels was simultaneously determined for p-Si ($\rho = 12\ \Omega$ cm), n-Si (NTD, 3 kΩ cm) and an Si:Ar$^+$ implanted layer by the algorithms discussed above. These results are demonstrated in table 1. It is important to point out that these values τ_b, s and D characterize (with a space resolution of 1 mm^2) only the local area of the wafer. The lateral variation of τ_{eff} is found to be different for various batches of wafers. For NTD wafers, values of τ_{eff} vary with lateral gradients of 0.1–1 μs mm^{-1} and an average value of $\tau_{\text{eff}} = 60\ \mu$s, while for wafers containing swirls defects these variations are greater than 3 μs mm^{-1} with an average value of 2 μs.

Table 1. Separated recombination parameters for wafers of various doping and preparation processes.

Wafer	s (cm s^{-1})	τ_b (μs)	D (cm^2 s^{-1})
p-Si KDB-12	10^4	70	18
n-Si NTD, oxidized	600	230	8
n-Si NTD etched	3.6×10^3	230	13
p-Si, unimplanted substrate	3.5×10^3	7	15
p-Si:Ar$^+$, Ar$^+ = 10^{13}$ cm^{-2} implanted layer	3.8×10^3	0.6	13
p-Si:Ar$^+$, Ar$^+ = 10^{16}$ cm^{-2} implanted layer	5×10^4	6×10^{-4}	0.015

Table 2. Comparison of τ_{eff} for CZ p-Si 10 Ω cm wafer ($d = 400$ μm) after different wafer preparation processes.

Process	τ_{eff} (μs)
Mechanical polishing	4.3
Lapped + HF etch	4.8
Chemo-mechanical polishing	6.7
Dislocations 10^3 cm^{-2}	6.0
Dislocations 10^7 cm^{-2}	2.5

Figure 8. Asymptotic lifetime (τ_{eff}) dependence on temperature in NTD Si measured at low and moderate excitation levels. Simulated dependences (curves) are obtained taking into account SRH recombination (τ_0) and the trapping effect (τ_M) respectively.

Figure 7. Asymptotic lifetime dependence on pulsed excitation intensity with and without additional steady-state illumination in NTD n-type and p-type 20 Ω cm Si wafers. Calculated dependences: according to equation (20) for n-Si (curve 1) and for p-Si (curve 2) according to equation (21).

5. Trapping impact

The most important feature of fast carrier trapping [15, 17] is the decrease of τ_{Mtr} with increasing excess carrier concentration as well as with steady-state additional illumination (figure 7, NTD Si). Such a dependence simulated according to equation (20) is presented by curve 1. It shows good quantitative correlation between experimental and calculated variation of τ_{Mtr}. The trapping coefficient $K \approx M/N_{\text{CM}}$ is obtained to be in the range of $K \approx 0.3$–1.2 for various oxidized and etched NTD

wafers at room temperature, and $K \geq 5$ at $T = 250$ K. The activation energy E_M of the traps is determined from the dependence of the trapping coefficient on the temperature (figure 8) in the range of temperatures $T = 250$–440 K. The temperature dependences of asymptotic lifetime were measured at moderate excitation pulse energy ($E_{\text{ex}} = 0.2$ μJ/pulse) to minimize the trapping effect and to afford MWA response registration where U_m decreases due to weaker absorption of the excitation light. Additionally, τ_{eff} was controlled for some temperatures at a low excitation level (0.07 μJ/pulse). It can be seen from figure 8 that the trapping effect is enhanced at low temperatures. The dependence $\tau_{\text{eff}}(T^{-1})$ for an oxidized wafer displays a maximum at about $T = 320$ K. The increase of τ_{eff} with temperature is found for an etched sample. Activation energy values $E_{\text{tb}} = 0.16 \pm 0.02$ eV and $E_{\text{ts}} = 0.20 \pm 0.02$ eV can be obtained from the experimental slope $\tau_{\text{eff}}(T^{-1})$ with corrections concerning carrier thermal velocity and density of states dependences on the temperature for both samples. For more precise separation of activation energy the simultaneous performance of several recombination centres as well as

the dependence of τ_b on excitation intensity must be considered, to give a more accurate correlation between experimental and simulated characteristics in figure 8. In our case the nonlinearity of recombination complicates such a type of extraction procedure. The simultaneous action of three recombination centres is accounted in the τ_{eff} (T^{-1}) simulation procedure. The parameters of the traps determined from DLTS measurements on these samples are included. The trapping effect due to deep levels is simulated by accounting for asymptotic lifetimes τ_M (equation (20)) dependences on temperature and excitation level, for a passivated sample. A similar model is used for an etched wafer when trapping at surface states (τ_{Ms}) take place. SRH-type recombination (equation (19)) is assumed for the system of two recombination levels. The simulated lifetime dependences on temperature can be considered as a qualitative model based on the trap system determined from DLTS. In a more precise model the processes of nonlinear trap filling via carrier redistribution should be taken into account as it includes more free parameters. The energy level $E_{\text{tb}} = 0.16$ eV identified from the slope $(kT)^{-1}\tau_{\text{eff}} = f(T^{-1})$ can be attributed to point defects [7, 19]. It was found to be $E_M \approx 0.28 \pm 0.04$ eV for trapping centres.

A trapping effect associated with the extended defects (i.e. increasing of τ_{eff} both with excitation intensity and AI) is also found (figure 7, p-Si). The characteristic of such trapping simulated according to equation (21) is presented by curve 2 in figure 7. Correlation between experimental (without AI) and calculated data is good in the ranges of low and high excitation. In the range of moderate excitation the impact of the dependence of τ_b on excitation intensity disturbs the appearance of the trapping effect. The geometrical cross section σ_0 is evaluated to be of the order of 10^{-10}–10^{-8} cm^2 from $\tau_{\text{Mtr}}(\Delta n)$ in the framework of this model.

6. Conclusions

The contactless microwave and infrared absorption methods are modified for the investigation of instantaneous decay characteristics and asymptotic recombination time (dependence on temperature, on excitation intensity and excitation depth). These techniques allow the competition between the recombination and trapping centres to be revealed and the parameters of bulk and surface recombination to be separated. They can be applied for express monitoring of lateral and depth striation of the grown-in and processing-induced recombination defects.

The nonlinearities of recombination processes must be accounted for in the analysis of recombination processes at moderate and high levels of excitation. Reconcilable experimental measurements and numerical simulations are necessary for the simultaneous determination of recombination parameters. Recombination parameters obtained by these investigations are in agreement with analogous ones determined by other methods.

References

[1] Luke K L and Cheng L J 1987 *J. Appl. Phys.* **61** 2282
[2] Waldmeyer J 1988 *J. Appl. Phys.* **63** 1977
[3] Grivickas V, Gaubas E, Kaniava A, Linnros J, Salmanov A R, Zemko A E, Travlejev G N, Kazakevich L A, Kuznecov V I and Filippov I M 1992 *Lith. J. Phys.* **32** 307
[4] Shimura F, Okui T and Kurama T 1990 *J. Appl. Phys.* **69** 7168
[5] Ling Z G and Ajmera P K 1991 *J. Appl. Phys.* **69** 519
[6] Norga G J, Black M R, Black K A, M'Saad H, Michel J and Kimerling L C 1995 *Mater. Sci. Forum* **196–201** 1531
[7] Aberle A G, Glunz S and Warta W 1992 *J. Appl. Phys.* **72** 442
[8] Vaitkus J, Gaubas E, Jarasiunas K and Petrauskas M 1992 *Semicond. Sci. Technol.* **7** A131
[9] Buczkowski A, Radzimski Z J, Rozgonyi G A and Shimura F 1992 *J. Appl. Phys.* **72** 2873
[10] Pang S K and Rohatgi A 1993 *J. Appl. Phys.* **74** 5554
[11] Goldner R B, Wong K K and Hass T E 1992 *J. Appl. Phys.* **72** 4674
[12] Gaubas E and Vanhellemont J 1996 *J. Appl. Phys.* **80** 1
[13] Vaitkus J, Gaubas E and Kaniava A 1992 *Lith. J. Phys.* **32** 434
[14] Kaniava A, Rotondaro A L, Vanhellemont J, Menczigar U and Gaubas E 1995 *Appl. Phys. Lett.* **67** 3930
[15] Ryvkin S M 1964 *Photoelectric Effects in Semiconductors* (New York: Consultants Bureau) ch 6
[16] Blakemore J S 1962 *Semiconductor Statistics* (Oxford: Pergamon) ch 8
[17] Vaitkus J and Vischakas J 1972 *Sov. Phys. Collect* **19** 421
[18] Yablonovitch E and Gmitter T 1986 *Appl. Phys. Lett.* **490** 586
[19] Maekawa T, Inoue S, Aiura M and Usami A 1986 *Semicond. Sci. Technol.* **1** 305